4ICEGE Thessaloniki-GREECE 2007

4th International Conference on
Earthquake Geotechnical Engineering
June 25-28, 2007
Paper No. 1141

LATERAL LOAD TESTING OF LARGE DRILLED SHAFTS AFTER BLAST-INDUCED LIQUEFACTION

Kyle ROLLINS [1], Seth BOWLES[2], Dan BROWN[3] and Scott ASHFORD[4]

ABSTRACT

Lateral statnamic load tests were performed on a 2.59 m diameter drilled shaft foundation at the Ravenel bridge site in Charleston, South Carolina after liquefying the soil to a depth of 13 m using controlled blasting. The damping ratio for the shaft in liquefied sand was between 30 and 35%. The static lateral resistance was interpreted from the statnamic test using a lumped mass approach. The interpreted static lateral resistance was very similar to that measured in hydraulic actuator tests on an adjacent test shaft at the same site. The interpreted static load-deflection curve indicates that the liquefied sand provided significant lateral resistance and that a reasonable estimate of the response could be obtained using LPILE with p-y curves for liquefied sand ($D_r \approx 50\%$) developed based on lateral load tests on piles in liquefied sand at Treasure Is. which consider the effect of pile diameter.

Keywords: Piles, Liquefaction, Field Load Test, Statnamic, Blast Liquefaction

INTRODUCTION

The lateral resistance of deep foundations in liquefiable sand has been an important issue in geotechnical earthquake engineering for many years. Approaches to evaluate lateral pile resistance in liquefiable sand have included centrifuge tests (Wilson et al., 2000), large scale shaking table tests (Suzuki and Tokimatsu, 2003) and full-scale field tests using blast induced liquefaction (Rollins et al. 2005a, Weaver et al. 2005). Centrifuge testing avoids the higher cost of full-scale or large scale testing and allows an examination of multiple factors involved. Nevertheless, full-scale field testing can be particularly helpful for site-specific investigations for important bridges in seismically active areas. This was certainly true for the Arthur Ravenel Bridge which now spans the Cooper River in Charleston, South Carolina, USA. Completed in July 2005, the Ravenel Bridge has a clear span of 471 m (1546 feet), making it the longest cable-stayed bridge in North and South America. Geotechnical investigations for the Ravenel Bridge determined that liquefaction could occur to a depth of 13 m on the eastern approach in a repeat of the 1886 Charleston earthquake (estimated M7.3). Based on the success of the Treasure Island Liquefaction Test (TILT) in San Francisco (Ashford et al 2004, Rollins et al 2005a, Weaver et al 2005), designers included full-scale blast liquefaction testing as part of the $4 million foundation testing program for the new bridge (Camp et al 2002). Following blast-induced liquefaction, lateral load tests were performed using both conventional hydraulic load actuators and a statnamic loading device to evaluate lateral resistance of the large diameter drilled shaft foundations anticipated for the bridge. This paper will focus on the test results obtained with the statnamic loading device. Comparisons will also be made with results from the TILT project in an effort to evaluate the effect of pile diameter on the lateral resistance of the liquefied sand.

[1] Prof., Civil & Env. Engrg Dept.. Brigham Young Univ.,Provo, UT USA Email: rollinsk@byu.edu
[2] Staff Engineer, Wright Engineers, Irvine, CA, USA. Email:seth.bowles@gmail.com
[3]Prof., Civil Engrg. Dept., Auburn Univ., Auburn, AL, USA Email: BROWND2@auburn.edu
[4] Prof. Struc. Eng. Dept., Univ. of California, San Diego, CA, USA Email: sashford@ucsd.edu

GEOTECHNICAL SITE CHARACTERISTICS

The soil profile at the test site generally consists of alluvial sands underlain by the Ashley formation of the Cooper Group at a depth of 13 to 14 m. This formation is known locally as the Cooper Marl. Groundwater was generally located between the ground surface and a depth about of 1.5 m, depending on tidal fluctuations. The sandy sediments of the coastal plain in South Carolina are typically loose Pleistocene age materials while the Cooper Marl is an Eocene to Oligocene age marine deposit. Prior to design of the bridge, a comprehensive geotechnical investigation was carried out to define the characteristics of the subsurface materials at the site. Preliminary studies were initially performed by Parson-Brinkerhoff and more detailed investigations were subsequently performed by S&ME, Inc. Based on the test hole logs, Camp et al (2002) developed an idealized soil profile for the site with six layers. This profile, with some minor modifications, is shown in Figure 1.

The first layer typically extends from the ground surface to a depth of 1.5 m and consists of loose, poorly graded fine sand (SP) to silty sand (SM). In some cases, sandy clay layers were interbedded in this material. The surface sand was typically underlain by a sandy clay layer 1.0 to 1.5 m thick which classified as CH material. This clay layer was very soft and had an average natural moisture content of about 106%, which is approximately the same as the liquid limit suggesting that the clay is normally consolidated. The PI was typically about 70%. The third layer was also a loose, fine sand (SP) to silty sand (SM) similar to the first layer and typically extended to a depth of 5.5 m. The fines content varied considerably with depth and from hole to hole with a range from 0.5 to 28%. The

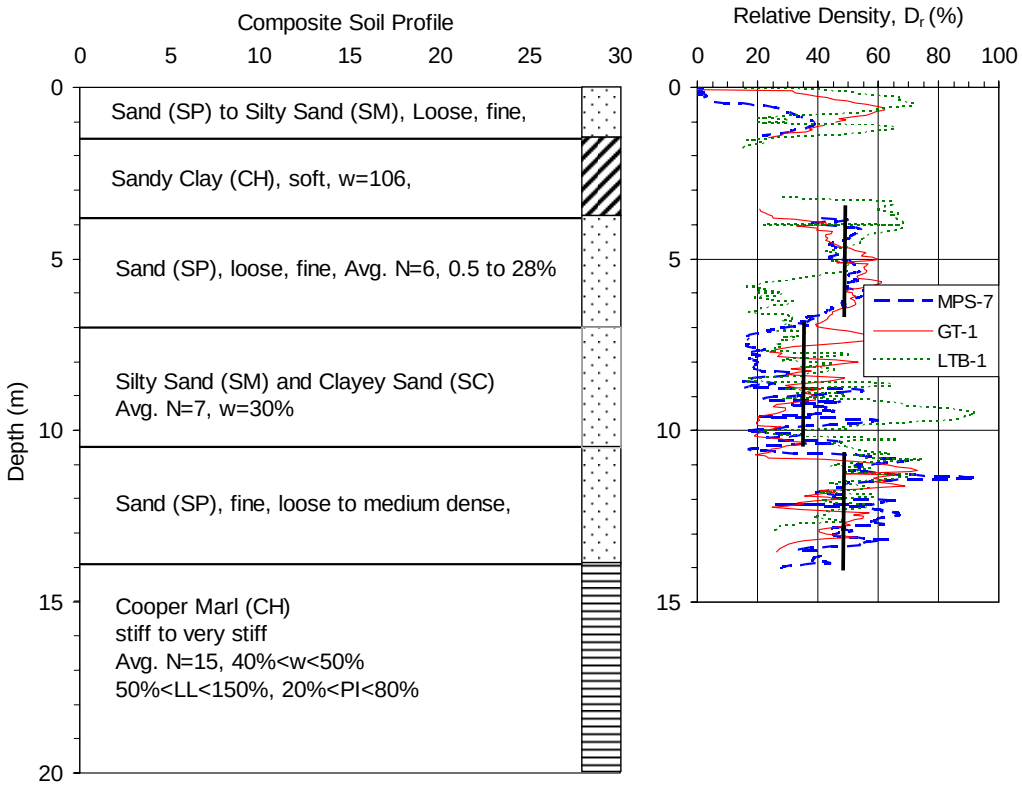

Figure 1. Idealized soil profile for the test site (Camp et al, 2002).

fourth layer was typically located between 5.5 and 8.5 m below the ground surface. This layer was also a sand layer but contained significantly more fines. The layer typically classified as silty sand (SM) or clayey sand (SC). The natural moisture content was 30% and the fines content varied from 15 to 24%. The fifth layer generally began at 8.8 m depth and extended to the top of the Marl. This layer

contained fewer fines and generally classified as a loose to medium dense poorly graded fine sand (SP).

The Cooper Marl was encountered between 12.8 m and 14 m below the ground surface and extended to a depth of 85 m, which was below the base of all the test foundations at the site. The Cooper Marl is a stiff, high plasticity calcareous silt or clay and generally classifies as MH or CH material (Camp et al 2002) according to the Unified Soil Classification System. The liquid limit typically ranges between 50 to 90% with a plasticity index varying from 15 to 60%. The natural moisture content is typically between 40 and 60% which is somewhat higher than the plastic limit but much lower than the liquid limit indicating overconsolidation. The marl is very stiff with undrained strengths typically ranging from 100 to 200 kPa at the top of the layer and increasing with depth to a value between 200 and 300 kPa at a depth of about 45 m. Below this depth, the strength appears to remain relatively constant.

Cone penetration (CPT) soundings were performed at several locations near the test area. The normalized cone tip resistance (q_{c1}) for three of these soundings was used to estimate the relative density (D_r) of the coarse-grained layers using the equation

$$D_r = \left[\frac{\left(\frac{q_{c1}}{p_a} \right)}{305} \right]^{0.5} \qquad (1)$$

developed by Kulhawy and Mayne (1990) for clean sands. The relative density profiles computed using Eq. 1 are also plotted in Figure 1. In two of the sand layers the average relative density is approximately 50%; while, in the silty sand layer the relative density drops to about 35%. However, Eq. 1 likely underestimates the relative density in this layer because of the silt content.

FOUNDATION CHARACTERISTICS AND TEST LAYOUT

Test Foundations

The test piles for the actuator test (MP-1) and the statnamic test (MP-3) were 2.59 m outside diameter, cast-in-steel-shell (CISS) piles. The steel casing, with a thickness of 25.4 mm, was advanced through the sand layers and into the Cooper Marl at a depth of 16.15 m using a vibratory hammer. The casing was then drilled out and the hole was advanced through the Marl to a depth of 47 m without casing. The hole was then filled with concrete using a tremie pipe. Based on 10 tests, the concrete had an average 30-day compressive strength of 37.2 MPa (5.4 ksi). The vertical reinforcement consisted of 36 #18 bars evenly distributed around a circle with a diameter of 2.14 m. Confinement for the vertical steel was provided by #6 bar spirals with a pitch of 89 mm. A 150 mm concrete cover was maintained between the spiral reinforcement and the inside of the steel case. A profile of the shaft with two cross-sections is provided in Figure 2.

Load Test Layout and Instrumentation

For the hydraulic actuator tests, the load was applied at a height of 0.533 m above the ground surface using two MTS actuators acting in parallel, each capable of producing 2200 kN of force. To provide a reaction, another pile with nearly identical properties was constructed approximately 8.5 m from test pile MP-1 on centers. The actuators were connected to each pile with a pinned connection to provide a free-head condition. This connection allowed the application of cyclic compressive and tensile forces. Each actuator was controlled with an electromechanical servo-valve and an electric hydraulic pump. Two LVDTs were set up to measure displacements of the pile head. They were mounted to a reference beam supported by driven piles within isolation casings. The LVDTs were attached to MP-1

at heights of 0.533, and 1.335 m above the ground surface. Therefore, the lower LVDT was in line with the point load application on MP-1. Four load cells on each of the two actuators provided a direct measurement of the applied load. Additional details regarding the hydraulic actuator tests are provided by Rollins et al (2005b).

For the statnamic load tests the load was applied at height of 1.31 m above the ground surface on shaft MP-3 as shown in Figure 3. The statnamic load sled weighed approximately 70 tons and was supported on a "runway" composed of steel H sections which were in turn supported by driven piles. A photograph of the statnamic load sled being moved into position with a crane prior to testing is presented in Figure 4. Applied load was measured by a load cell on the piston section and pile head deflection was measured using LVDTs. In addition, two accelerometers were attached to the pile head so that deflection could be determined by double integration. In addition, a string of eight downhole accelerometers were installed at depths shown in Figure 2 within an inclinometer cast into the test shaft

Prior to concrete placement, resistance-type strain gages were mounted on "sister bars" composed of a 0.9 m long #4 bars and tied into the rebar cage at 10 depth intervals. At each strain gauge station, two strain gauges were mounted on opposite sides of the pile separated by a distance of about 2.14 m. The gauges were oriented to be in line with the direction of loading. Figure 2 also shows the strain gauge locations on pile MP-3 and their depths below ground. All of the pile data (load, deflection, acceleration and strain) was monitored via a data acquisition system.

To quantify the build-up and dissipation of pore pressure after blasting, 20 piezometers were installed at various distances and depths around the test pile. The location and depth of each piezometer are shown in Figure 5. Basically, three vertical arrays were installed at radii of 1.83, 7.32 and 10.36 m from the center of the test pile. All the piezometers were distributed around the front of the pile in the direction of loading to track the variation in pore water pressure with applied load. Transducers identified with a B employed piezoresistive transducers identical to those at Treasure Island (Ashford et al, 2004) while those identified with an A used electrical resistance transducers (Rollins et al 2005c). The electrical resistance transducers were more sensitive to damage during blasting and several transducers closest to the explosive charges were damaged during blasting while those further from the charges provided some useful information. Additional information regarding pore pressure transducer selection, installation, and performance is provided by Rollins et al (2005c).

Liquefaction is manifest by an increase in pore water pressure. This increase in pore water pressure was achieved by detonating explosive charges distributed around MP-3 test shaft. A pilot liquefaction test was performed at a location separate from the test site for MP-3 to better define the charge weight, spacing, and delay sequence necessary to produce liquefaction. For each of the load tests, eight charges spaced evenly around three different radii were detonated. The first eight blast holes were spaced around a radius of 3.96 m. The second and third blast rings radii were 4.57 m and 5.18 m, respectively. The charges were staggered to help avoid sympathetic detonations. The first blast series used a 0.68 kg (1.5 lb) charge at 3.05, 6.1, 9.14, and 11.73 m below the ground surface. The second blast series used 0.91 kg (2 lb) charges at 4.57, 7.62, and 10.67 m depths. The third and final blast series put 0.68 kg (1.5 lb) charges at the same depths as in the first blast series. The blast hole layout is also shown in Figure 6. The binary explosives consisted of a mixture of ammonium nitrate and nitro-methane, and the weights are given in equivalent weights of TNT. During each of the three blast sequences, the charges were detonated two at a time with a delay of 250 milliseconds. between detonations. The charges were detonated beginning around the bottom ring and then moved upward around each subsequent ring to the top.

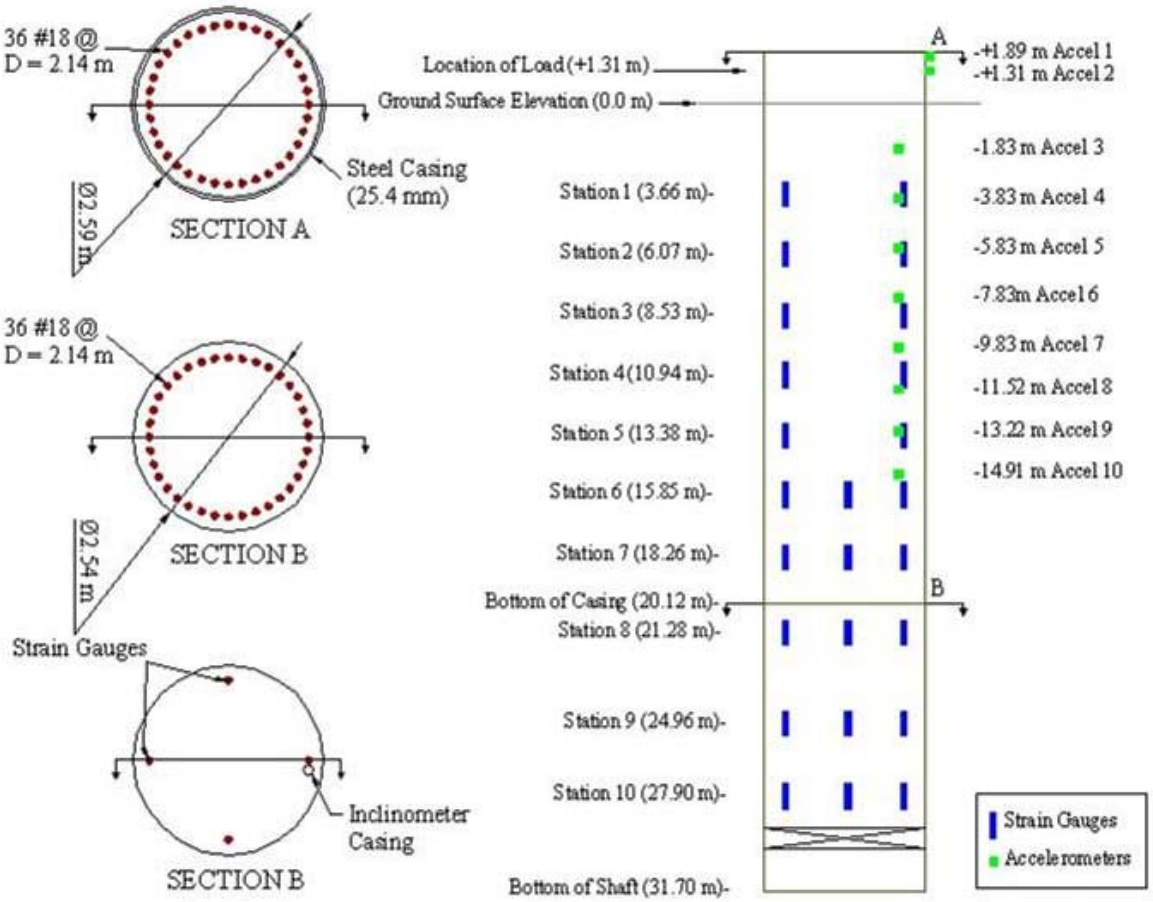

Figure 2. Profile and cross-sections through test shaft

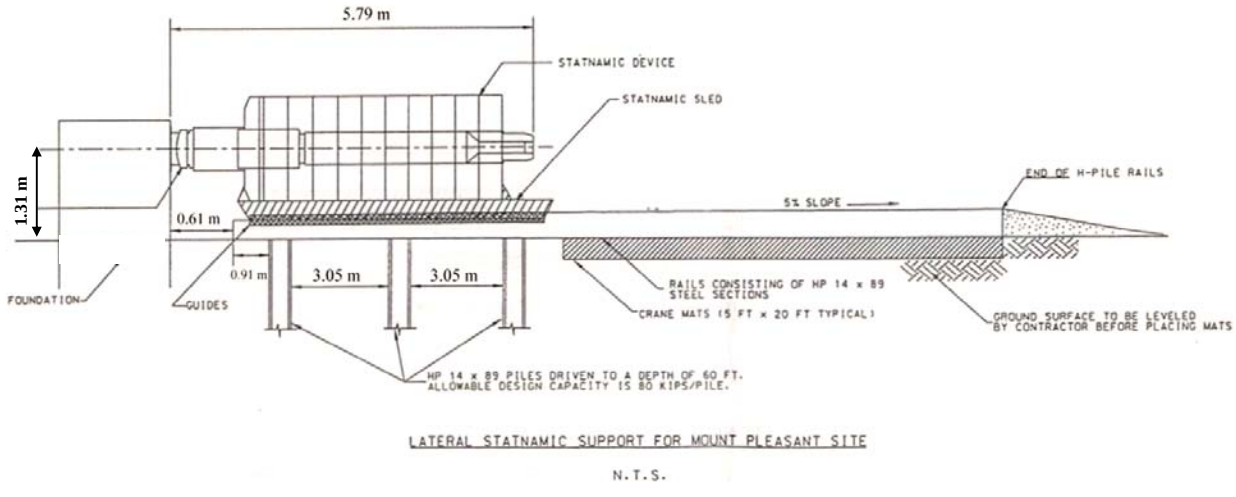

Figure 3. Test setup for lateral statnamic load tests.

Figure 4. Photograph of statnamic load sled being moved into position for load test.

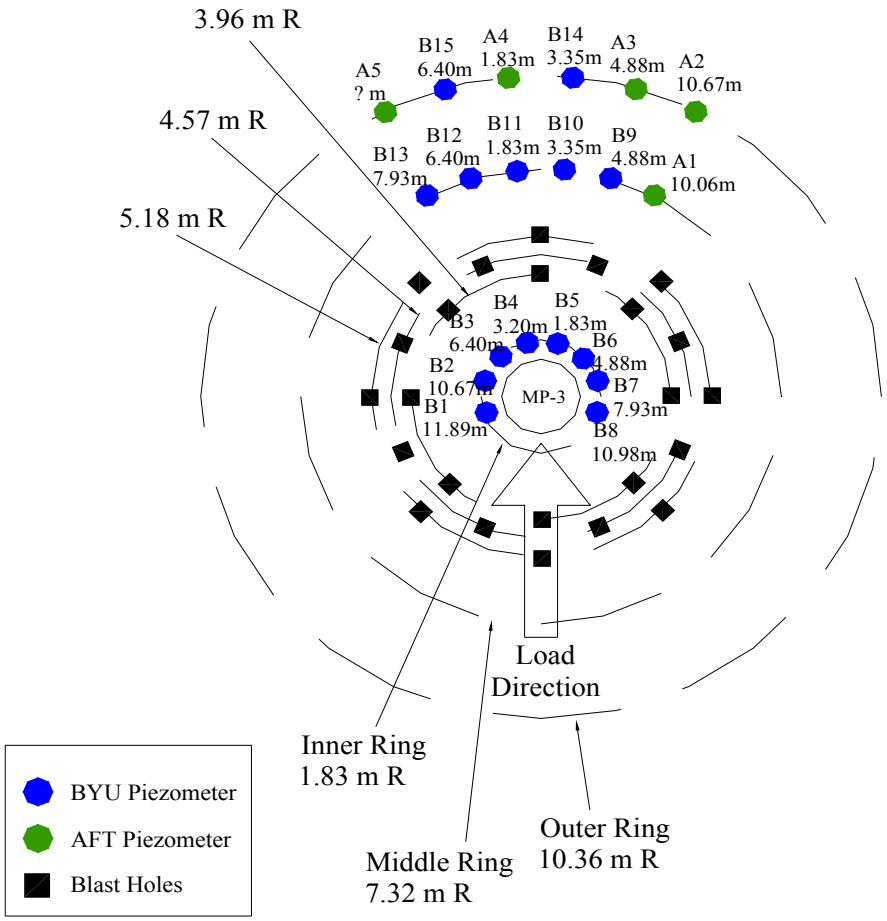

Figure 5. Plan view with layout of blast holes and piezometers relative to test shaft.

STATNAMIC LATERAL LOAD TEST RESULTS

Blast Liquefaction

Prior to each statnamic lateral load test, the explosive charges were detonated as described previously. After a period of about 30 seconds to allow gases from the blast holes to vent, the fuel pellets in the statnamic load sled were ignited. The excess pore water pressures developed by the charges were measured by each piezometer and normalized to facilitate comparison using the expression

$$R_u = \frac{u_f - u_i}{\sigma'_o} \tag{2}$$

where u_f is the piezometer reading of pore water pressure during testing, u_i is the measured pore water pressure prior to blasting, and σ'_o is the initial vertical effective stress in the soil prior to blasting. The vertical effective stress was calculated using a moist unit weight above the water table of 17.75 kN/m^3 and a saturated unit weight of 19.97 kN/m^3 below the water table which was at a depth of 1.52 m during testing. As can be seen in Eq. 1, when the excess pore water pressure increases and equals the effective stress, $R_u = 1.0$ or 100% and the soil is fully liquefied.

While the piezoelectric piezometers generally performed well, many of the electrical resistance type piezometers were apparently damaged during the blasting and did not provide reliable data. A plot of the peak residual excess pore pressure ratio versus depth for each ring of piezometers is provided in

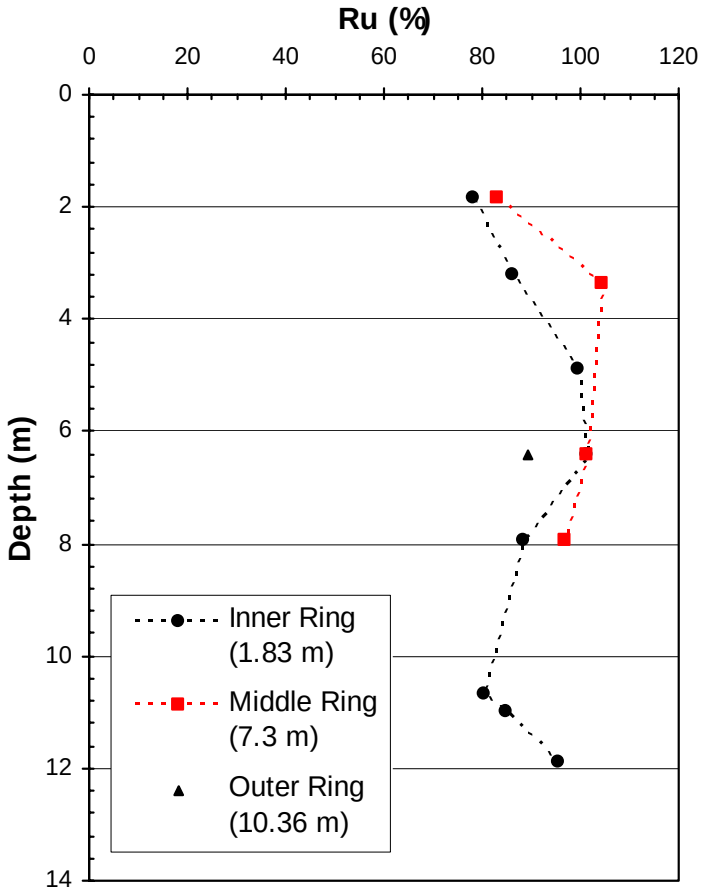

Figure 6. Peak excess pore pressure ratio versus depth profiles from three rings of piezometers during the first statnamic test.

Figure 6. The residual R_u values were typically between 80 and 100%. There appears to be a tendency for lower R_u values at 2 to 3 m below the ground surface. The lower R_u values could be explained by the fact that this layer consisted of clay zones which would be less susceptible to liquefaction.

Load-Displacement Response

Time histories of load and deflection for the second statnamic load test are presented in Figure 7. The rise time for the applied load was approximately 0.1 second, while the total duration of loading was about 0.27 seconds. As the load level increased for a given test, the rise time decreased. The peak deflection occurred some time after the peak load. In fact, the applied load is only about 10% of the maximum load when the peak deflection occurs. Although this loading does not strictly correspond to "free-vibration" conditions, it is close enough that an estimate of the damping ratio can be obtained using the log-decrement method. Based on this approach the damping ratio for the three statnamic load tests was estimated to be between 0.30 and 0.35.

The dynamic load versus deflection curve for the second statnamic load test is shown in Figure 8. In contrast to dynamic tests involving an eccentric mass shaker where deflections are on the order of a few millimeters, the peak deflection during the statnamic test exceeded 85 mm.

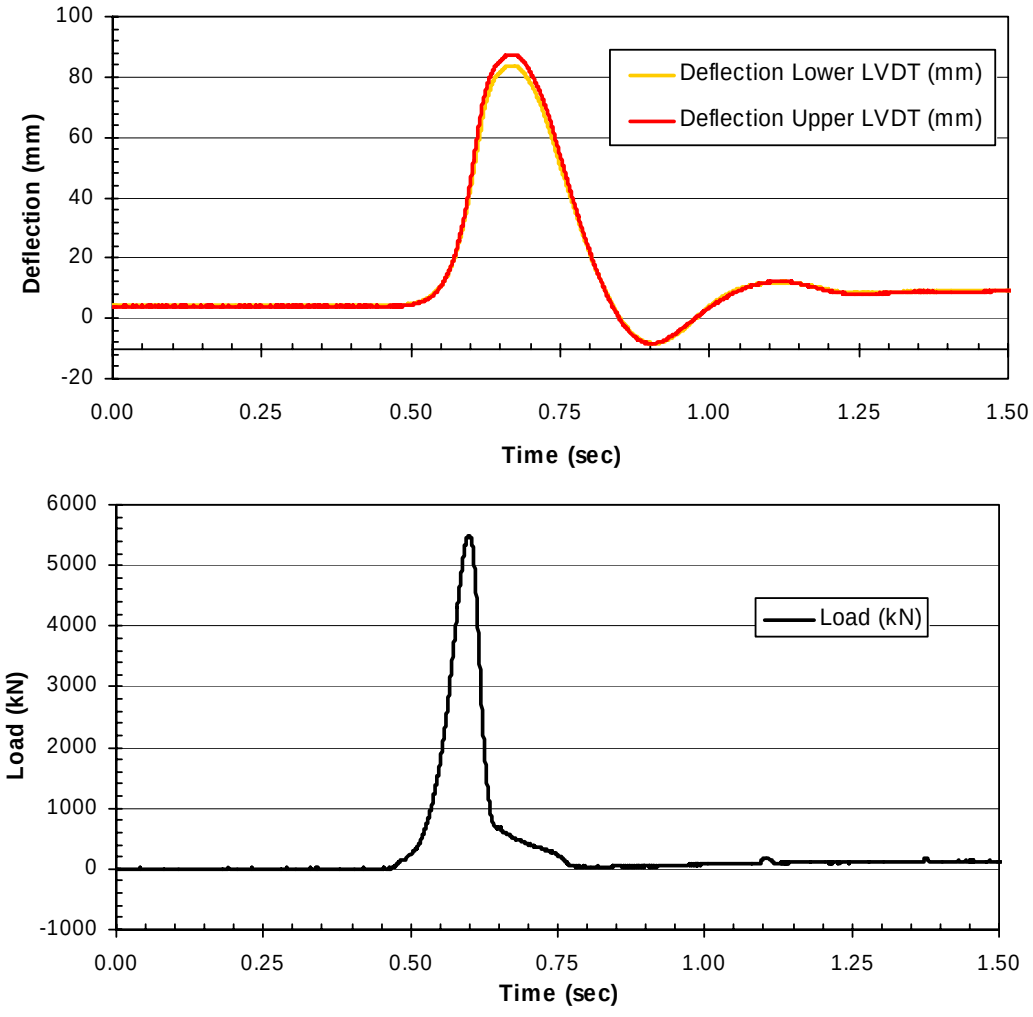

Figure 7. Time histories of load and deflection for the first statnamic lateral load test.

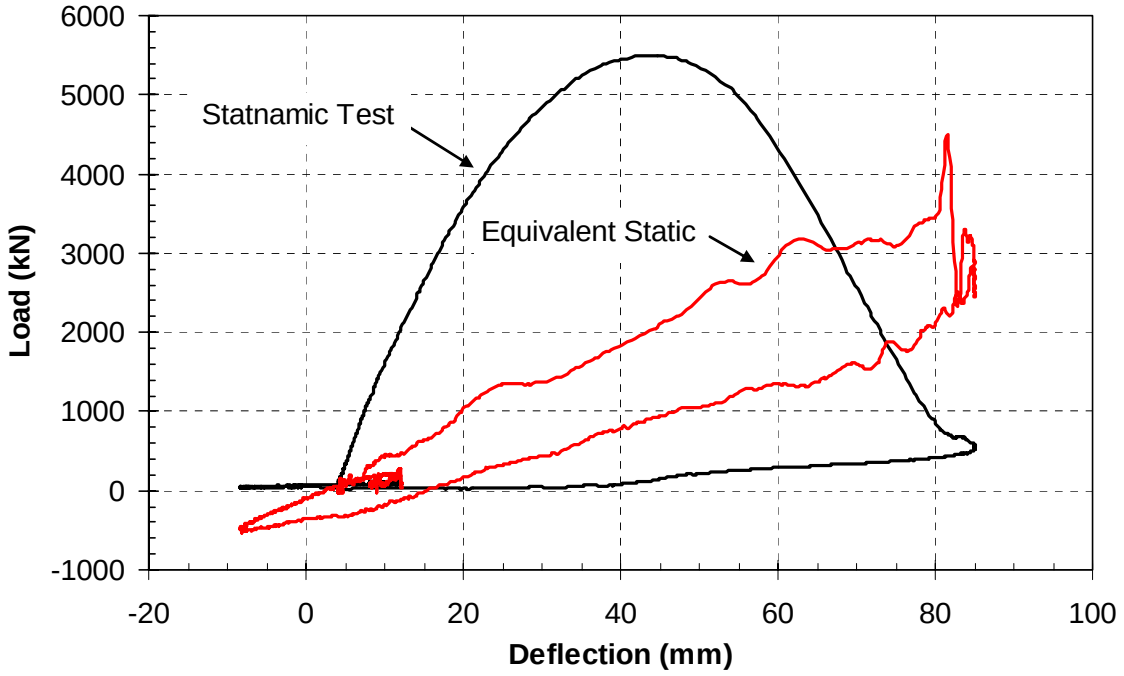

Figure 8. Dynamic load versus deflection curve for second statnamic load test along with interpreted equivalent static load versus deflection curve.

ANALYSIS OF TEST RESULTS

The load measured by the statnamic load cell (F_{stn}) includes the contribution to load provided by inertia (F_i), damping (F_d), and static soil resistance (F_s) as given by the equation

$$F_{stn} = F_i + F_d + F_s \tag{3}$$

The large loop in the load versus deflection curve indicates that damping is a significant component of the total load. Expressions for the inertia and damping forces based on a lumped-mass approximation can be substituted into Eq. 3 to obtain the expression

$$F_{stn} = \Sigma M_i a_i + \Sigma C_i v_i + F_s \tag{4}$$

where M_i is the mass of a given segment of the shaft, a_i is the acceleration of the segment, C_i is the damping coefficient for the segment, and v_i is the velocity of the segment. The static lateral force provided by the soil-shaft system could then be obtained using the equation

$$F_s = F_{stn} - \Sigma M_i a_i - \Sigma C_i v_i \tag{5}$$

if the inertia and damping forces could be subtracted from the statnamic force. Because the acceleration was measured at 8 depth intervals along the shaft as well as at the top of the shaft, the inertia force could be readily determined as a function of time during each statnamic test. In addition, the acceleration time histories at each depth could be integrated to obtain velocity time histories for each segment of the shaft. The most significant difficulty lies in estimating an appropriate damping coefficient. For this study, this value was estimated based on the log-decrement method as discussed previously. Using Eq. 5, the interpreted static lateral resistance versus deflection curve for the second statnamic test was determined and it is plotted in Figure 8. In comparison with the dynamic load versus deflection curve, the static curve is far more linear as expected. Although the contribution to load provided by damping is substantial, the analyses indicate that the contribution provided by inertia

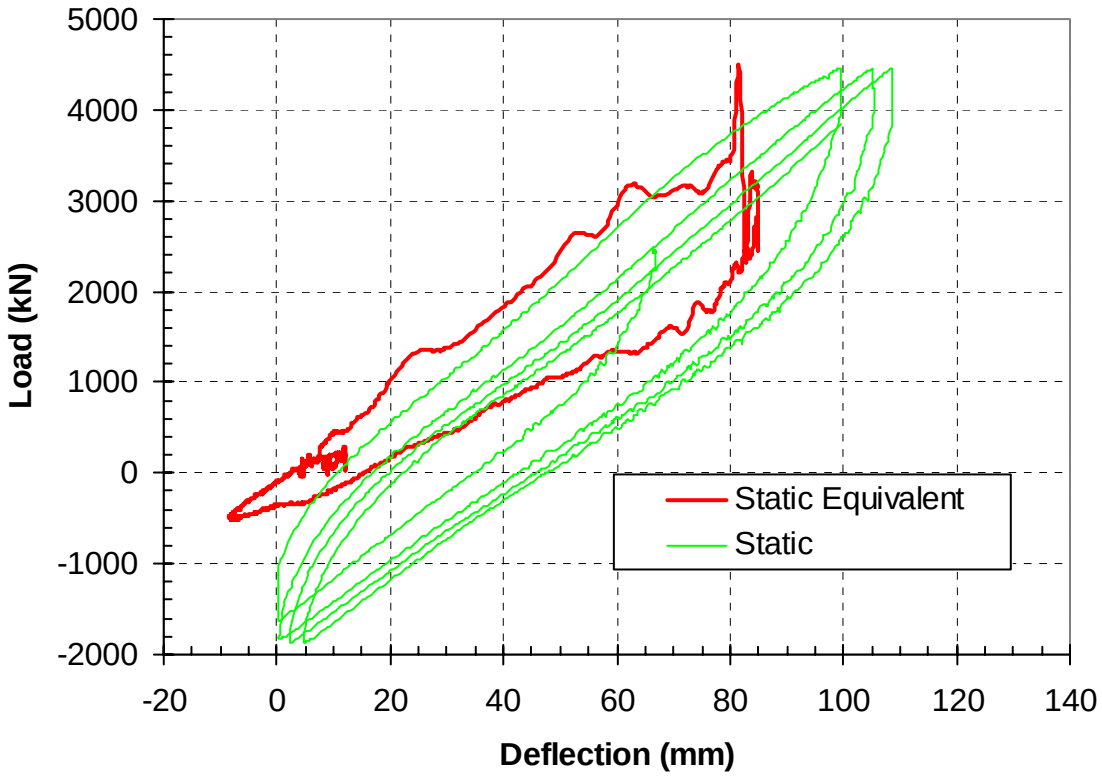

Figure 9. Comparison of equivalent static load versus deflection curve interpreted from the statnamic lateral load tests in comparison with curve from static load test using hydraulic actuators (Rollins et al, 2005b).

is far greater. The interpreted static load vs. deflection curve from the statnamic test is compared with the static load versus deflection curve obtained from the lateral load tests performed using hydraulic actuators on test shaft MP-1 in Figure 9. Although the curves are offset due to a difference in the initial starting point for the static load test, the slope of both curves is remarkably similar. In addition, the shape of the load-unload loop for both curves is also similar. These similarities suggest that the damping ratio used to interpret the static load-deflection curve from the statnamic test is reasonable.

Based on the Treasure Island liquefaction tests, Rollins et al (2005a) developed the equation

$$p = A\,(By)^{C} p_d \qquad (6)$$

to define the lateral soil pressure per length of pile (p) in kN/m in liquefied sand as function of horizontal pile deflection y in mm. This equation was developed for sands with D_r of about 50%, while sands with a D_r of about 35% were found to produce essentially no resistance. In Eq. 6, $A = 3x10^{-7}(z+1)^{6.05}$, $B = 2.80(z+1)^{0.11}$, $C = 2.85(z+1)^{-0.41}$, z = depth in meters and $p_d = 3.81\ln d + 5.6$ where d is the pile diameter in meters. To evaluate the applicability of this equation for the Charleston load tests, lateral pile load analyses were carried out using the computer program LPILE plus version 5.0.12 (Reese et al, 2004). The p-y curve shapes, layer thicknesses and soil properties used in the analyses are summarized in Table 1. Within the liquefied zone, two cases were investigated. For the first case, the resistance in the entire liquefied zone (3.5 to 12.5 m) was considered to be zero, which is a worst case situation. For the second case, the resistance in the liquefied zone was assumed to be zero when the D_r was 35%, but was defined by Eq. 6 when D_r was about 50%. The load versus deflection curve computed for the first case assuming no resistance in the liquefied zone is much softer than the measured curve obtained from field testing. However, the curve computed for the second case where the p-y curves in the liquefied sand were based on Eq. 6 with a p_d value of about 9.0, the computed load-deflection curve agrees favourably with the measured curve.

Table 1. Soil properties used in the lateral pile load analysis with LPILE.

Depth interval	p-y Curve Shape	γ	ϕ	K	C	ε_{50}
		kN/m^3	Degrees	MN/m^3	kN/m^2	
0-1.5 m	API Sand (API, 1983)	19.5	38	58.5	0	-
1.5–3.5 m	Soft Clay (Matlock, 1970)	10.0	0	-	Linear 25 to 50	0.02
3.5 -7.0 m	Liquefied Sand (D_r=50%) (Rollins et al, 2005)	9.5	Resistance from Eq. 6			
7.0-10.5 m	Liquefied Sand (D_r=35%) (Rollins et al, 2005)	9.5	No Resistance			
10.5-12.5 m	Liquefied Sand (D_r=50%) (Rollins et al, 2005)	9.5	Resistance from Eq. 6			
12.5-31.7 m	Cooper Marl (Reese et al, 1975)	10.15	0	135.7	207	0.005

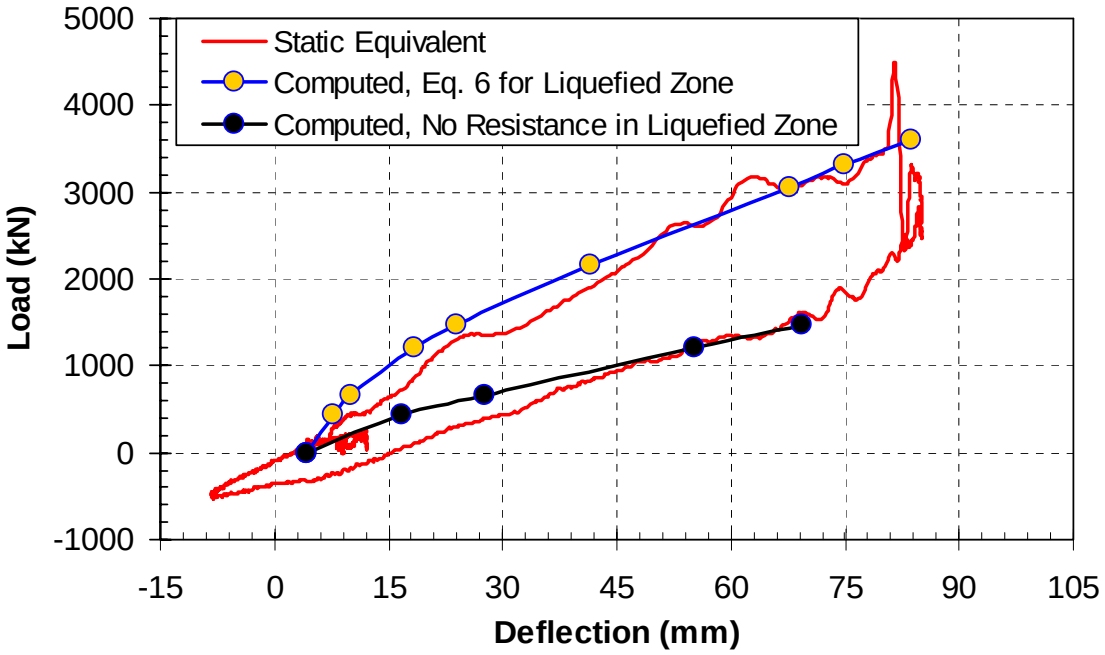

Figure 10. Comparison of interpreted load versus deflection curve with curves predicted by LPILE assuming (a) no soil resistance in liquefied zone and (b) p-y curves for liquefied sand in Dr=50% sand proposed by Rollins et al (2005a).

CONCLUSIONS

1. The blast liquefaction technique in combination with the statnamic lateral load procedure provides a viable means for evaluating the dynamic lateral resistance of deep foundations in liquefied sand under full-scale conditions. These tests can be particularly valuable in evaluating foundation behaviour for important structures.
2. The interpreted static lateral resistance from the statnamic test using a lumped mass approach was approximately the same as the static lateral resistance measured in hydraulic actuator tests on an adjacent test shaft at the same site.
3. The damping ratio for the 2.59 m diameter drilled shaft in liquefied sand during the statnamic testing was approximately 30 to 35%.

4. The interpreted static load-deflection curve indicates that the liquefied sand provided significant lateral resistance and that a reasonable estimate of the response could be obtained using p-y curves for liquefied sand ($D_r \approx 50\%$) developed by Rollins et al (2005a) which include diameter effects.

AKNOWLEDGEMENTS

Funding for the full-scale load tests was provided by the South Carolina Department of Transportation and Modern Continental South was the contractor for the testing program. Applied Foundation Testing installed the strain gages, piezometers, and LVDTs and was responsible for data acquisition. Financial support for the analysis of the test results was provided by the National Science Foundation under Grant No. CMS-0085353. This funding is gratefully acknowledged. Nevertheless, the opinions and conclusions in this paper do not necessarily reflect the views of the sponsors.

REFERENCES

American Petroleum Institute [API]. (1993). Recommended Practice for Planning, Designing, and Constructing Fixed Offshore Platforms. API RP @A-WSD, 20th Edition.

Ashford, S.A., Rollins, K.M., and Lane, J.D. (2004) "Blast-induced liquefaction for full-scale foundation testing," *J. Geotechnical and Geoenvironmetal Engrg*., ASCE, Vol. 130, No. 8, 798-806.

Camp, W.M., Brown, D.A., and Mayne, P.W. (2002). "Construction method effects on axial drilled shaft performance" *Deep Foundations 2002, Geotechnical Special Publication No. 116*, ASCE, Vol. 1, p. 193-208.

Kulhawy, F. H., and Mayne, P. W. (1990). Manual on estimating soil properties for foundation design. Research Project 1493-6, EL-6800, Electric Power Research Institute. Palo Alto, California.

Matlock, H. (1970). "Correlations for Design of Laterally-Loaded Piles in Soft Clay" *Procs., Second Annual Offshore Technology Conf.*, Paper No. OTC 1204, Vol. 1, 577-594.

Reese, L.C., Cox, W.R., and Koop, F.D. (1975). "Field Testing and Analysis of Laterally Loaded Piles in Stiff Clay", *Proceedings*, Offshore Technology conference, Houston, Texas, Paper No. 2312, pp. 671-690.

Reese, L.C., Wang, S.T., Isenhower, W.M. and Arrellaga, J.A. (2000). "Computer program LPILE plus version 5.0 users manual", Ensoft, Inc., Austin, Texas.

Rollins, K.M., Gerber, T.M., Lane, J.D. and Ashford. S.A. (2005a). "Lateral resistance of a full-scale pile group in liquefied sand," *J. Geotechnical and Geoenvironmental Engrg*., ASCE, Vol. 131, No. 1, p. 115-125.

Rollins, K.M., Hales, L.J., Ashford, S.A. and Camp, W.M. III (2005b). "P-Y Curves for Large Diameter Shafts in Liquefied Sand from Blast Liquefaction Tests", *Geotechnical Special Publication No. 145, Seismic Performance and Simulation of Pile Foundations in Liquefied and Laterally Spreading Ground*, Ed. Boulanger, R.W. and Tokimatsu, K., ASCE, p. 11-23.

Rollins, K.M., Lane, J.D., Dibb, E., Ashford, S.A., Mullins, A.G. (2005c). "Pore pressure measurement in blast-induced liquefaction experiments," *Transportation Research Record 1936*, "Soil Mechanics 2005", Transportation Research Board, Washington DC, p. 210-220.

Suzuki, H. and Tokimatsu, K. (2003). "Effect of pore water pressure response around pile on p-y relation during liquefaction," Procs. 11th Intl. Conf. on Soil Dynamics and Earthquake Engineering, Stallion Press, Vol. 2, p. 567-572.

Weaver, T.J., Ashford, S.A. and Rollins, K.M. (2005) "Lateral resistance of a 0.6 m drilled shaft in liquefied sand," *J. Geotechnical and Geoenvironmental Engrg.*, ASCE Vol. 131, No. 1, p. 94-102.

Wilson D.W., Boulanger, R.W. and Kutter, B.L (2000). "Observed Seismic Lateral Resistance of Liquefying Sand", *Journal of Geotechnical and Geoenvironmental Engineering*, Vol. 126, No. 10, October 2000, pp. 898-906.